ALCHEMY Jurnal Penelitian Kimia

Official Website: https://jurnal.uns.ac.id/alchemy

ISSN 1412-4092
EISSN 2443-4183

Kinetics and Thermodynamics Equilibrium of Nickel Metal Ions Sorption onto Carbon Nanofibers Irradiated by Ultrasonic Energy

Alimin Alimin[a*], La Ode Ahmad Nur Ramadhan[a], La Ode Ahmad[a], Fahmiati Fahmiati[a], Darwin Ismail[a], Ahmad Zaeni[a], Muhammad Zakir Muzakkar[a], Intan Intan[a], La Agusu[b], Indriana Kartini[c], and Sri Juari Santosa[c]

[a]*Department of Chemistry, Universitas Halu Oleo*
Kampus Hijau Bumi Tridharma, Anduonohu, Kendari, 93232, Indonesia.
[b]*Department of Physics, Universitas Halu Oleo*
Kampus Hijau Bumi Tridharma, Anduonohu, Kendari 93232, Indonesia.
[c]*Department of Chemistry, Universitas Gadjah Mada,*
Sekip Utara, Bulaksumur, Sendowo, Caturtunggal, Depok, DI Yogyakarta, 55281, Indonesia

[*]*Corresponding author: aliminkim91@uho.ac.id*

DOI: 10.20961/alchemy.20.1.74223.22-30

Received 26 May 2023, Revised 20 December 2023, Accepted 21 December 2023, Published 30 March 2024

Keywords:

carbon nanofibers
nickel;
kinetics;
thermodynamics;
ultrasonic.

ABSTRACT. In this work, we investigated the effects of the heavy metal initial concentration and the pH on the sorption of heavy metal ions onto carbon nanofibers using the liquid phase adsorption technique under ultrasonic energy irradiation. These data were then used to study thermodynamic aspects such as sorption capacity and energy and kinetic parameters such as kinetic model, reaction order, and rate constant of heavy metal sorption on carbon nanofibers. We found that the increase of the heavy metal (nickel) initial concentration was proportional to the amount of heavy metal adsorbed onto carbon nanofibers. The highest uptake of the heavy metal ions' amount onto carbon nanofibers in equilibrium (q_e) was 244.00 mg.g^{-1}, achieved at the pH of 8. Langmuir and Freundlich's isotherms were used to find the best-fitted isotherms model. The Langmuir isotherm best fits the sorption equilibrium of the heavy metal ions on Carbon nanofibers. Both pseudo-first and pseudo-second orders studied the sorption and kinetic parameters of heavy metals on carbon nanofibers. The sorption kinetics model was fitted to the pseudo-second-order. Based on the value of Gibbs free energy, the metal ions' sorption onto carbon nanofibers occurs spontaneously.

INTRODUCTION

Southeast Sulawesi is one of the biggest nickel mines in Indonesia. The metal is widely used in various industries, such as nickel-based batteries, metallurgical operations, electroplating, plastics manufacturing, and lead framing. Unfortunately, those industry activities generate numerous environmental impacts, for instance, pollution of the water environment. It is well known that nickel ions (Ni^{+}) are carcinogenic metal ions because in high concentrations, their ingestion can cause numerous health problems, such as lung and kidney damage and stomach problems, *e.g*., diarrhea, renal edema, vomiting, *etc*. (Fila *et al.*, 2019; Kumar *et al.*, 2019; Shahriari *et al.*, 2019). To overcome this problem, many attempts have been made to enhance effective and efficient methods for removing Ni^{2+} metal ions from aqueous solutions. The adsorption technique is the most popular method because of its ease of operation, high efficiency, low pollution, and low cost. Various adsorbents have been applied successfully to uptake nickel ions pollutants, such as biomaterials (Akinyeye *et al.*, 2016; Charazińska *et al.*, 2021; Cruz-Lopes *et al.*, 2022; Kristianto *et al.*, 2019), nanofibrous membranes composite (Olufemi and Omolola, 2018; Thangaraj *et al.*, 2019; Zafar *et al.*, 2019; Zhang and Wang, 2015), metal oxide nanoparticles (Aijaz *et al.*, 2021; Fato *et al.*, 2019), carbon materials (Salihi *et al.*, 2016) and its composite (Lin *et al.*, 2021). Allotropes of carbon such as carbon nanotubes, graphene oxide, and carbon nanofibers (CNFs) are adsorbents that have been intensively used not only for removing heavy metals such as lead, copper, zinc, and iron ions (Alimin *et al.*, 2018; Lin *et al.*, 2021; Nordin *et al.*, 2020; Salihi *et al.*, 2016; Zakaria *et al.*, 2021) but also nickel ions in wastewater (Abdullah and

Cite this as: Alimin A., Ramadhan, L.O.A.N., Ahmad, L.O., Fahmiati, F., Ismail, I., D., Zaeni, A., Muzakkar, M.Z., Intan, I., Agusu, L., Kartini, I., & Santosa, S.J., 2024. Kinetics and Thermodynamics Equilibrium of Nickel Metal Ions Sorption onto Carbon Nanofibers Irradiated by Ultrasonic Energy. *ALCHEMY Jurnal Penelitian Kimia*, 20(1), 22-30. https://dx.doi.org/10.20961/alchemy.20.1.74223.22-30.

Rinaldi, 2015). Among these carbon allotropes, CNFs have been attracted incredible attention from researchers who concerned with metal ions removal from aqueous solution (Abdullah and Rinaldi, 2015; Mubarak *et al*., 2017; Nordin *et al.*, 2020; Zakaria *et al.*, 2021) because it has large specific surface area, pore volume, and proper functionalities (Abd Wahab *et al.*, 2016; Abdullah and Rinaldi, 2015; Alimin *et al*., 2022). Therefore, in the present work, we selected CNFs to remove nickel ions from an aqueous solution for studying the kinetics and thermodynamics equilibrium of nickel metal ions sorption on the nanocarbon.

Interaction between metal ions and an adsorbent in an aqueous solution is conventionally assisted by magnetic stirring. However, in recent years, ultrasound irradiation has extended more attention to numerous applications (Alimin *et al.*, 2018; Alimin *et al.*, 2022; Alimin *et al.*, 2015; Ramutshatsha-Makhwedzha *et al.*, 2019). It is believed that ultrasonic energy is powerful enough to assist not only metal ion uptake by an adsorbent but also metal ion reduction onto adsorbent such as CNFs (Alimin *et al.*, 2018; Alimin *et al.*, 2022; Alimin *et al*., 2015). Due to the pressure wave propagation through the liquid, ultrasound irradiation can assist in accelerating the chemical process via the formation of acoustic cavitation (Roosta *et al.*, 2014). The process generates the collapse and growth of bubbles on a micrometer scale produced by pressure waves supporting the process of strengthening mass transfer. Moreover, the process will enable the interaction between sorbents such as CNFs and sorbates such as metal ions, which will then be directed to improve adsorption (Asfaram *et al.*, 2015). Hence, in this work, we applied ultrasonic energy to assist the sorption of nickel ions on CNFs, which was intensively used in the adsorption process.

This work investigates nickel ions' kinetics, thermodynamics, and sorption isotherm parameters on CNFs assisted by ultrasonic energy. The following experimental parameters, such as sonication time, pH, and initial concentration of nickel ions affecting the metal ions sorption on CNFs, were optimized for studying kinetics and thermodynamics equilibrium of the sorption process as objectives of this work.

RESEARCH METHODS

All chemicals selected in this work were analytical grade with high purity. $Ni(NO_3)_2{\cdot}6H_2O$ 98.5 wt% (E. Merck), Carbon nanofibers (CNFs) we purchased from the sigma Aldrich, NaOH and HCl (E. Merck), Whatman Millipore 0.45 μm, Analitical balance (Vibra AJ-420g), 370 pH Meter Jenway, Atomic Absorption Spectrometer (Hitachi Z-2000).

Procedures

The methods used in this study were referred to in our previous work (Alimin *et al.*, 2018). Briefly, the effect of contact time on the nickel ions sorption was studied by doping $Ni(NO_3)_2{\cdot}6H_2O$ solution on CNFs assisted by an ultrasonic wave of 53 Hz (BAKU BK-2000) in various sonication times of 10, 15, 30, 60, 120, and 210 minutes. The effect of initial pH on the sorption of metal ions was studied in various pH of 2, 3, 5, 8, 9, and 11, assisted by ultrasonic energy for 120 minutes. All pH measurements used a pH meter (370 pH Meter Jenway), and HCl or NaOH solutions were used to adjust the initial pH levels of the experimental solution. The effect of the initial concentration of the metal ions on the adsorption was studied through interaction between CNFs and the metal ions with different concentrations of $Ni(NO_3)_2{\cdot}6H_2O$ solution for 120 minutes under a pH of 8. All separation processes between the adsorbent and the solution in this work used 0.45 pore size Whatman membrane filter paper. Contents of nickel ions that were not incorporated in CNFs were determined by an atomic absorption spectrometer (Hitachi Z-2000). Contents of the metal ions adsorbed onto CNFs were calculated from the difference between the contents of the initial and the metal ions remains. All the calculated parameters of kinetics and thermodynamics equilibrium of the metal ions sorption onto CNFs, such as the amount of the ions uptake, maximum sorption capacity (q_m), sorption energy ($\sim\Delta G^o$), mechanism and sorption rate, and sorption isotherms refer to our previous work (Alimin *et al.*, 2018). The amount of the metal ions uptake onto CNFs at equilibrium, qe (mg/g), is given by Equation (1).

$$q_e = \frac{(C_o - C_e) \times V}{M} \quad (1)$$

C_o and C_e (mg/L) are the liquid phase concentration of the metal ions at the initial and equilibrium states, respectively; V (L) is the volume of solution; and M (g) is the mass of dried CNFs used. The content of metal ions' uptake into CNFsi was calculated using Equation (2).

$$Contents\ of\ metal\ ions\ uptake\ (\%)\ =\ \frac{(C_o-C_e)}{C_o}\times 100 \quad (2)$$

The procedure of contact time effect as adsorption kinetics aspect in this study was similar to batch equilibrium. However, the amount of the metal ions adsorbed in CNFs at equilibrium, q_e (mg/g), is obtained by calculating the metal ions' uptakes at selected time intervals. The amount of the adsorbed metal ions at any time, q_t (mg/g), was calculated by Equation (3).

$$q_t = \frac{(C_o - C_t)\times V}{M} \quad (3)$$

For studying adsorption isotherms, both Langmuir and Freundlich's models were fitted in this work. Langmuir adsorption isotherm is given by Equation (4).

$$\frac{C_e}{q_e} = \frac{1}{q_m K_L} + \frac{C_e}{q_m} \quad (4)$$

The label q_m (mg/g) notes the maximum adsorption capacity and K_L is Langmuir equilibrium constant. R_L associated with characteristics of Langmuir isotherm is determined by Equation (5).

$$R_L = \frac{1}{(1+q_m K_L)} \quad (5)$$

Freundlich adsorption isotherm is given by Equation (6).

$$\log q_e = \log K_F + \frac{1}{n}\log C_e \quad (6)$$

K_F (mg.g^{-1})(L.g^{-1})$^{1/n}$ is the Freundlich constant associated with adsorption capacity. The number of 1/n (mg.L^{-1}) is the Freundlich constant corresponding to the sorption intensity of the sorbent.

The adsorption kinetics analysis is crucial because it indicates the rate at which the adsorbate is uptake by an adsorbent. The mechanism and rate of nickel ions adsorption onto CNFs can be determined based on kinetic analysis. For studying the sorption kinetics, pseudo-first-order and pseudo-second-order models were used according to Equations (7) and (8), respectively.

$$\log(q_e - q_t) = \log q_e - \frac{k_1}{2.303}t \quad (7)$$

$$\frac{t}{q_t} = \frac{1}{k_2 q_e^2} + \frac{t}{q_e} \quad (8)$$

The labels k_1 (min^{-1}) and k_2 (g. g^{-1}.min^{-1}) represent the sorption rate constant of pseudo-first-order and pseudo-second-order.

RESULTS AND DISCUSSIONS

Sorption Behavior of Nickel Metal Ions onto CNFs

The effect of sonication time is demonstrated in Figure 1. The percentages of nickel ions uptake increases with the increasing entire contact times. However, nickel ions' uptake sharply increases at the first region of contact time, ranging from 10 to 20 min. Nickel ions' sorption is slightly increased in the second region of contact time from 20 to 60 min. The equilibrium was achieved at 120 min and was expressed in the occupation on the sorbent surface of the remaining active sites. The percentage of nickel ions' uptake at a contact time of 120 min was nearly the same as the amount of the metal ions' uptake at 210 min, i.e., 88.21 %. Sonications time of 120 min was considered the optimum contact time. The high amount of metal ions adsorbed onto CNFs may be attributed to the high abundance of active sites and the large specific surface area of the sorbent (Abdullah and Rinaldi, 2015; Alimin *et al*., 2018; Alimin *et al*., 2022; Gouda and Aljaafari, 2021). In addition, the pressure wave propagation

through liquid generated by ultrasound energy may assist in activating the surface area of CNFs. It implies that ultrasound tends to favor interacting with CNFs rather than nickel ions. As a result, the affinity of CNFs to nickel ions tends to increase even for long contact time.

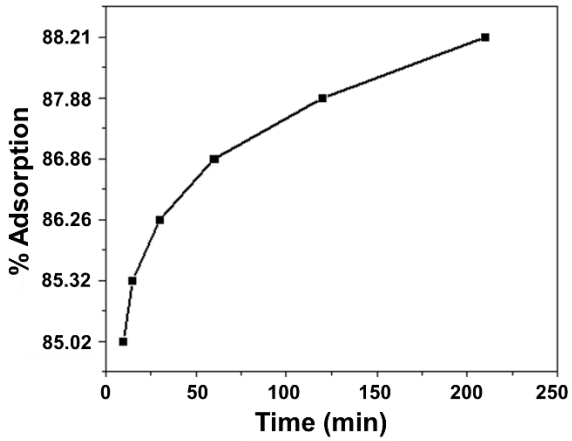

Figure 1. The effect of sonications time on the amount of nickel ions uptake on CNFs

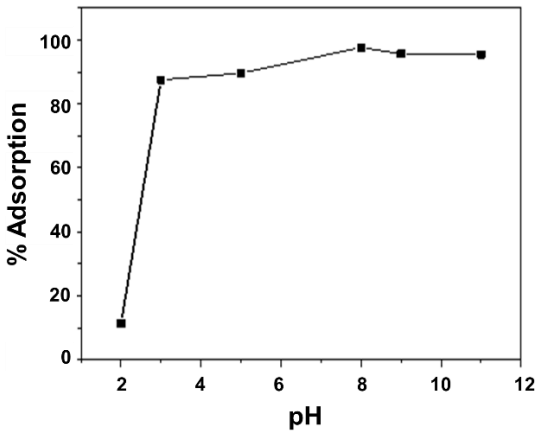

Figure 2. The effect of initial pH on the amount of nickel ions uptake on CNFs

Figure 2 shows the effect of different initial pH ranges from 2 to 11 on the sorption of nickel ions onto the sorbent. Figure 2 reveals that the sorption of the metal ions increased as the pH value dramatically increased from 2 to 3. The lower metal ions' uptake at the lowest pH (pH=2) is attributed to the high abundance of hydronium ions (H_3O^+) protonating CNFs' surface. The positive charge of hydronium ions protonated CNFs active sites will prevent interaction between nickel ions and the active sites. In addition, in an aqueous solution, the hydronium ions should compete with nickel ions to interact with CNFs' active sites.

Consequently, the amount of nickel ions adsorbed onto active sites of CNFs became lower. Nickel ions' uptake gradually increased at pH regions above two due to the increasing abundance of OH^- ions that were simultaneously followed by the decreasing concentration of hydronium ions. It will allow nickel ions to interact with CNFs' active sites. Therefore, the amount of the nickel ions uptake onto CNFs gradually increased. It almost became a plateau at pH interval ($3 < pH < 5$) and slightly increased at pH above 5. The optimum nickel ions uptake was achieved at a pH of 8 with a percentage of 97.6 %. Afterward, the uptake of metal ions gradually decreased at the pH region above 8. With the decreasing percentage of metal ions due to the high abundance of OH^- ions in solution, CNFs will compete with OH^- ions to interact with Ni^{2+} ions. The interaction between OH^- ions and Ni^{2+} ions in aqueous solution may create several species of nickel such as Ni^{2+}, $NiOH^+$, $Ni(OH)_{2(aq)}$, and $Ni(OH)^{3-}$. When the pH was above 8, Ni^{2+} was initiated to reduce, and the Ni species of $NiOH^+$ and $Ni(OH)_{2(aq)}$ commenced to be produced. When the pH was around 10, the occupied Ni species was Ni $(OH)_{2(aq)}$, while $Ni(OH)^{3-}$ began to be formed and disappeared when the pH was above 13 (Li *et al*., 2021). This fact suggested that the pH of the solution had a substantial effect on the hydrolyzed species of Ni ions. Hence, the suitable pH for studying the sorption of Ni ranged from 1 to 10 because most Ni ions would precipitate when the pH was above 10. The adsorption behavior of nickel species in various pH levels of aqueous solution onto the adsorbent was good, in agreement with the work of Li *et al*. (2021). However, in our work, even though at a pH of 11, the uptake of nickel ions was still relatively high. This phenomenon indicated that nickel species were stagnant in soluble nickel ions, and the precipitant of nickel hydroxide had not yet been produced. Ultrasonic energy also plays a vital role in preventing contact between some OH^- ions and nickel ions, and then early precipitation would be inhibited.

Kinetics Sorption

Both kinetic models, pseudo-first-order and pseudo-second-order, were applied to examine the effect of changing the adsorption time on the adsorption rate, as shown in Figures 3 and 4. These models were valuable for understanding the sorption of Ni^{2+} ions onto CNFs. Figure 3 shows the log plot ($qe - qt$) versus t, giving a straight line with ($-k_1/2.303$) as the slope and log q_e as the intercept. The values of sorption rate constant (k_1) and correlation coefficient (R^2) obtained from the plots of the metal ions sorption on the CNFs were 0.02073 min^{-1} and 0.973, respectively. Figure 4 presents the plot of t/q_e versus t and provides a straight line with $1/q_e$ as the slope and $1/k_2$

q^2_e as the intercept. The values of k_2 and R^2 obtained from the plots of the metal ions sorption on the CNFs were 0.004 g.mg^{-1}.min^{-1} and 0.999, respectively. Since the correlation coefficient (R^2) value of the pseudo-second-order model is nearly one that is much higher than the R^2 value of the pseudo-first-order model, the sorption experiment strongly coincides with the pseudo-second-order model (Kamatchi *et al*., 2022; Lin *et al*., 2021; Salihi *et al*., 2016). This model is one of the kinetic models based on the assumption that the rate-limiting step is chemical sorption or chemisorption (Al-Abbad and Al Dwairi, 2021). It is well known in chemical sorption that the presence of the active sites on the surface of a sorbent plays an essential role in the sorption process. Therefore, in this study, the sorption rate for the nickel ions strongly depends on the availability of CNF sites on the surface of the sorbent.

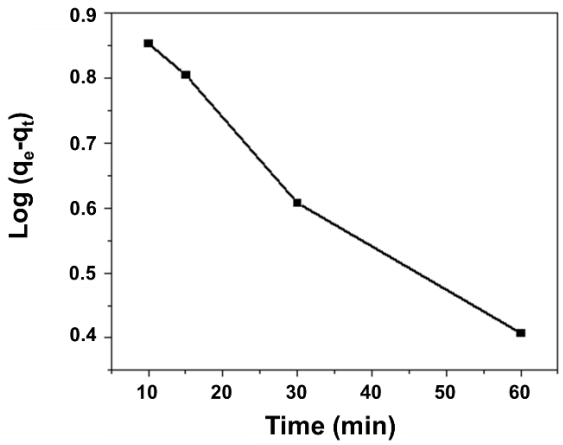

Figure 3. Pseudo-first order-kinetic model for Ni^{2+} metal ion sorption

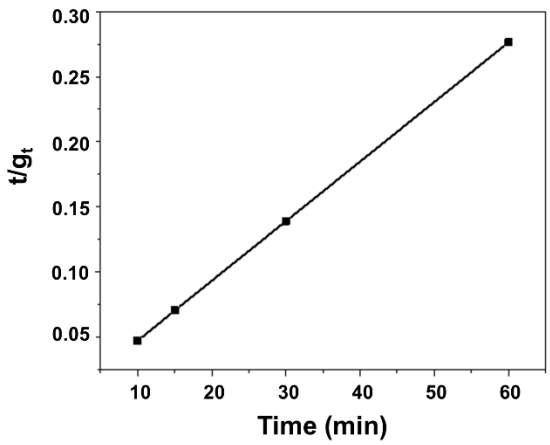

Figure 4. Pseudo-second-order-kinetic model for Ni^{2+} metal ions sorption

Due to the sorption data following the pseudo-second-order model, the q_e value can be calculated from the slope of the graph in Figure 4, in which the calculated value of q_e was 250 mg.g^{-1}. In this work, however, the calculated value of q_e was higher than the experimental value of q_e, i.e. 219.70 mg.g^{-1}. The experimental value of q_e was obtained by equation (1) using data of the optimum contact time of 120 min. i.e. C_o = 25 mg/L, M = 0.005 g, C_e = 3.0305 mg/L and V = 0.05 L. Kinetic parameters for sorption of Ni^{2+} ions onto CNFs in this work compared to other workers using the pseudo-second-order model were tabulated in Table 1. We selected reference having similar temperature experiment for comparing this work with other workers related to sorption isotherm and kinetic parameters for the Ni^{2+} sorption onto various type sorbents.

Table 1. Comparison of kinetic parameters for sorption of Ni^{2+} ions onto different sorbent applying Pseudo-Second-Order Model

Sorbents and References	Pseudo-Second-Order Model			Reference
	k_2 (g.mg^{-1}.min^{-1})	q_e (mg.g^{-1})	R^2	
Carbon Nanofibers (CNFs)	4×10^{-3}	219.70	0.999	Our work
Chloroxylon Swietenia Activated Carbon (CSAC)	1.17×10^{-4}	51.1389	0.999	Kamatchi *et al*., 2022
β-Cyclodextrin@Fe_3O_4/MWCNT (***β***-CD@Fe_3O_4/MWCNT)	8.63×10^{-4}	108	0.989	Lin *et al*., 2021
Graphene Oxide (GO)	1×10^{-4}	18.08	0.998	Salihi *et al*., 2016
Sodium Dodecyl Sulphate-Graphene Oxide (SDS-GO)	3.2×10^{-4}	32.05	0.997	Salihi *et al*., 2016

Table 1 shows that the sorption rate of nickel ions on the other sorbents was around 1×10^{-4} till 8×10^{-4} g.mg^{-1}.min^{-1}. In our work, however, the sorption rate was much higher than that for other sorbents. In addition, the q_e value of this sorbent was much higher than the q_e value for other sorbents.

Sorption Isotherms

Langmuir and Freundlich's models assessed the adsorption isotherms in this work. Figures 5 and 6 demonstrate curves of Langmuir and Freundlich adsorption isotherms, respectively. The straight line in Figure 5

was gained by plotting C_e/q_e versus C_e using Langmuir adsorption isotherm (Equation 4). The q_m value is determined through the slope of the straight line (Figure 5). In this case, the slope was expressed by $1/q_m$, and the intercept was $1/q_mK_L$. The characteristic of Langmuir isotherm can be evaluated by R_L value as Equation (5). The equilibrium data were fitted to both Langmuir's and Freundlich's isotherms. The q_m, K_L, R^2, and R_L values as Langmuir isotherm parameters were obtained. The values of those parameters are q_m (316.456 mg/g), K_L (0.1505 L/mg), R^2 (0.981), and R_L (0.0021).

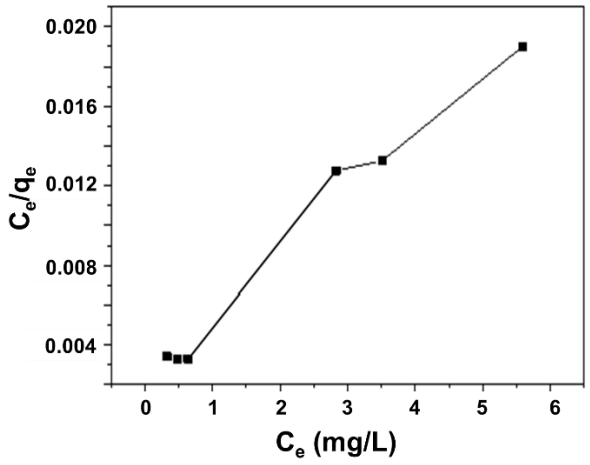

Figure 5. Langmuir isotherm for Ni^{2+} metal ions sorption

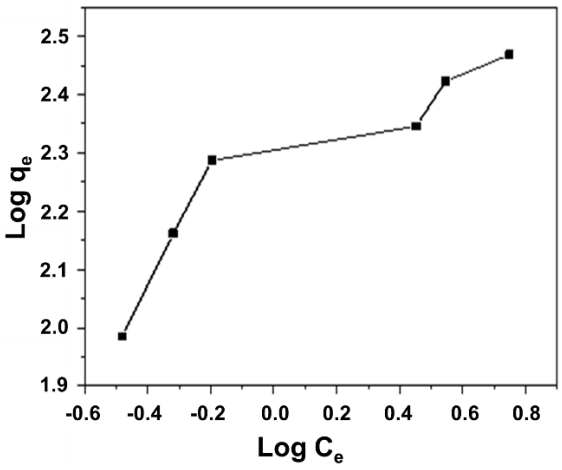

Figure 6. Freundlich isotherm for Ni^{2+} metal ions sorption

Figure 6 shows a plot of log q_e against log C_e, which provides a straight line taken from the Freundlich adsorption isotherm (Equation 6) with a slope of 1/n and an intercept of log q_m. The 1/n is the Freundlich constant corresponding to sorbent intensity, whereas K_f is the Freundlich constant related to adsorption capacity. The Freundlich isotherm parametersare $1/n_F$ (0.319 mg/L), K_F ((173.226 $mg.g^{-1}$) $(L.g^{-1})^{1/n}$), and R^2 (0.848). All crucial parameters of sorption isotherm for the Ni^{2+} sorption onto different sorbents compared to this work were tabulated in Table 2.

Table 2. Sorption isotherm parameters for the Ni^{2+} sorption onto different sorbents

Kinetic Models	Isotherm Parameters	Sorbents and Reference				
		CNFs (Our work)	CSAC (Kamatchi *et al*., 2022)	***β***-CD@Fe_3O_4/ MWCNT (Lin *et al*., 2021)	GO (Salihi *et al*., 2016)	SDS-GO (Salihi *et al*., 2016)
Langmuir isotherm	$q_m(mg.g^{-1})$	316.456	50.074	119	20.19	55.16
	K_L (L/mg)	0.1505	0.213	0.2737	0.32	0.40
	R^2	981	0.997	0.9924	0.990	0.992
	R_L	0.0021	0.0857	-	-	-
Freundlich isotherm	K_F $(mg.g^{-1})$ $(L.g^{-1})^{1/n}$	173.226	12.928	26.16	8.76	22.03
	R^2	0.848	0.971	0.9187	0.911	0.960

As shown in Table 2, in particular, the value of Langmuir isotherm's correlation coefficient (R^2) was higher than those of Freundlich isotherm. It can be inferred that nickel ion adsorption onto CNFs was the best fit with the Langmuir model. It suggests that the maximum adsorption of Ni^{2+} metal ions occurred covered by a monolayer of the adsorbate. In addition, due to the value of R_L being much less than 1, it then suggested that Langmuir adsorption isotherm is favorable for nickel ion sorption onto CNFs (Alimin *et al.*, 2018; Gouda and Aljaafari, 2021).

A thermodynamics parameter that was mainly determined in this study was Gibbs free energy (ΔG^o). It was determined by the Equation of $\Delta G^\circ = -RT \ln K$, in which the K value was obtained by K_L of Langmuir isotherm. ΔG° obtained in this work was -1.0294 $kJ.mol^{-1}$, suggesting that nickel sorption onto CNFs takes place spontaneously. In this case, Gibbs free energy is associated with sorption energy. Even though the capacity of the sorbent in this work compared to others was a finding of this study.

CONCLUSIONS

In the present work, we have investigated the kinetics and thermodynamics equilibrium of nickel metal ions sorption onto CNFs irradiated by ultrasound waves. We found that the sorption equilibrium of the metal ions on the sorbent was achieved at a sonication time of 120 min under the pH of 8. Ultrasound energy plays a vital role in enhancing the sorption capacity of CNFs on the metal ions. The sorption equilibrium tends to follow the Langmuir isotherm model. Based on Langmuir isotherm, we found that the maximum sorption capacity (q_m) and sorption energy (~ΔG^o) of the metal ions on CNFs were 316.456 $mg.g^{-1}$ and -1.029 $kJ.mol^{-1}$, respectively. In addition, sorption mechanisms of nickel metal ions onto carbon nanofibers tend to occur via chemisorption. Both pseudo-first and pseudo-second orders examined the sorption kinetics parameters of the heavy metal on CNFs. We obtained that the kinetics coincided nicely with the pseudo-second-order having a sorption rate constant (k) of 0.004 $g.mg^{-1}.min^{-1}$.

CONFLICT OF INTEREST

There is no conflict of interest in this article.

AUTHOR CONTRIBUTION

AA: Manuscript Drafting, Funding Acquisition; LOANR: Supervision; LOA: Methodology; FF: Data Analysis; DI: Editing; AZ: Validation; MZM: Tools Software (EndNote); II: Investigation; LA: Visualization for drawing graphical abstract; IK: Conceptualization; SJS: Manuscript Review

ACKNOWLEDGMENTS

We thank the Dean of the Mathematic and Natural Sciences Universitas Halu Oleo faculty and the Head of Biology and Chemistry Laboratories for using the AAS instrument.

REFERENCES

Abd Wahab, N. W., Sufian, S., Van, T. D. N., and Shaharun, M. S., 2016. Comparative Studies of Pristine and Functionalized CNFs Surface Properties and their Performance in Iron Distribution, *Procedia engineering*, 148, 136–145. https://doi.org/10.1016/j.proeng.2016.06.546.

Abdullah, N., and Rinaldi, A., 2014. Synthesis and Adsorption Performance of Carbon Materials for the Removal of Iron (III) from Aqueous Solution. *Presented at Applied Mechanics and Materials*., 699, 988–993. https://doi.org/10.4028/www.scientific.net/AMM.699.988.

Aijaz, M. O., Karim, M. R., Alharbi, H. F., Alharthi, N. H., Al-Mubaddel, F. S., and Abdo, H. S., 2021. Magnetic/Polyetherimide-Acrylonitrile Composite Nanofibers for Nickel Ion Removal from Aqueous Solution, Membranes, 11(1), 50. https://doi.org/10.3390/membranes11010050.

Akinyeye, O. J., Ibigbami, T. B., and Odeja, O., 2016. Effect of Chitosan Powder Prepared from Snail Shells to Remove Lead (II) Ion and Nickel (II) Ion from Aqueous Solution and Its Adsorption Isotherm Model. *American Journal of Applied Chemistry*, 4(4), 146–156. https://doi.org/10.11648/J.AJAC.20160404.15.

Al-Abbad, E. A, and Al Dwairi, R. A,. 2021. Removal of Nickel (II) Ions from Water by Jordan Natural Zeolite as Sorbent Material. *Journal of Saudi Chemical Society*, 25(5), 1–10. https://doi.org/10.1016/j.jscs.2021.101233.

Alimin, Agusu, L., Ahmad, L., Kadidae, L., Ramadhan, L., Nurdin, M., and Isdayanti, N., 2018. Kinetics and Equilibrium of Fe^{3+} Ions Adsorption on Carbon Nanofibers. *Presented at IOP Conference Series: Materials Science and Engineering*, 367(1), 1–6. https://dx.doi.org/10.1088/1757-899X/367/1/012046.

Alimin, A., Kadidae, L., Agusu, L., Ahmad, L., Santosa, S., and Asria, A., 2022. Formation Mechanisms of Co-existence of α-Fe and Iron Oxides Nanoparticles Decorated on Carbon Nanofibers by a Simple Liquid Phase Adsorption-Thermal Oxidation. *Journal of New Materials for Electrochemical Systems*, 25(3), 200–205. https://doi.org/10.14447/jnmes.v25i3.a07.

Alimin, A., Narsito, N., Kartini, I., and Santosa, S. J., 2015. Production of Silver Nanoparticle Chains inside Single Wall Carbon Nanotube with a Simple Liquid Phase Adsorption. *Bulletin of Chemical Reaction Engineering & Catalysis*, 10(3), 266–274. http://dx.doi.org/10.9767/bcrec.10.3.8416.266-274.

Asfaram, A., Ghaedi, M., Hajati, S., Goudarzi, A., and Bazrafshan, A. A., 2015. Simultaneous Ultrasound-Assisted Ternary Adsorption of Dyes onto Copper-Doped Zinc Sulfide Nanoparticles Loaded on Activated Carbon:

Optimization by Response Surface Methodology. *Spectrochimica Acta Part A: Molecular and Biomolecular Spectroscopy*, 145, 203–212. http://dx.doi.org/10.1016/j.saa.2015.03.006.

Charazińska, S., Burszta-Adamiak, E., and Lochyński, P., 2022. Recent Trends in Ni (II) Sorption from Aqueous Solutions Using Natural Materials. *Reviews in Environmental Science and Bio/Technology*, 21, 105–138. https://doi.org/10.1007/s11157-021-09599-5.

Cruz-Lopes, L., Macena, M., Esteves, B., and Santos-Vieira, I., 2022. Lignocellulosic Materials Used as Biosorbents for The Capture of Nickel (II) in Aqueous Solution. *Applied Sciences*, 12(2), 933–950. https://doi.org/10.3390/app12020933.

Fato, F. P., Li, D.-W., Zhao, L.-J., Qiu, K., and Long, Y.-T., 2019. Simultaneous Removal of Multiple Heavy Metal Ions from River Water Using Ultrafine Mesoporous Magnetite Nanoparticles. *ACS omega*, 4(4), 7543–7549. https://doi.org/10.1021/acsomega.9b00731.

Fila, D., Hubicki, Z., and Kołodyńska, D., 2019. Recovery of Metals from Waste Nickel-Metal Hydride Batteries Using Multifunctional Diphonix Resin. *Adsorption*, 25(3), 367–382, https://doi.org/10.1007/s10450-019-00013-9.

Gouda, M., and Aljaafari, A., 2021. Removal of Heavy Metal Ions from Wastewater Using Hydroxyethyl Methacrylate-Modified Cellulose Nanofibers: Kinetic, Equilibrium, and Thermodynamic Analysis. *International Journal of Environmental Research and Public Health*, 18(12), 6581–6597. https://doi.org/10.3390/ijerph18126581.

Kamatchi, C., Arivoli, S., and Prabakaran, R., 2022. Thermodynamic, Kinetic, Batch Adsorption and Isotherm Models for the Adsorption of Nickel from an Artificial Solution Using Chloroxylon Swietenia Activated Carbon. *Physical Chemistry Research*, 10(3), 315–324.

Kristianto, H., Daulay, N., and Arie, A. A., 2019. Adsorption of Ni (II) Ion onto Calcined Eggshells: A Study of Equilibrium Adsorption Isotherm. *Indonesian Journal of Chemistry*, 19(1), 143–150. https://doi.org/10.22146/ijc.29200.

Kumar, A., Balouch, A., Pathan, A. A., Jagirani, M. S., Mahar, A. M., Zubair, M., and Laghari, B., 2019. Remediation of Nickel Ion from Wastewater by Applying Various Techniques: A Review. *Acta Chemica Malaysia*, 3(1), 1–15. http://dx.doi.org/10.2478/acmy-2019-0001.

Li, C., Zhao, J., and Zhang, Y., 2021. Study on Adsorption Behavior of Nickel Ions Using Silica-Based Sandwich Layered Zirconium-Titanium Phosphate Prepared by Layer-by-Layer Grafting Method. *Nanomaterials*, 11(9), 2314. https://doi.org/10.3390/nano11092314.

Lin, S., Zou, C., Liang, H., Peng, H., and Liao, Y., 2021. The Effective Removal of Nickel Ions from Aqueous Solution onto Magnetic Multi-Walled Carbon Nanotubes Modified by B-Cyclodextrin, *Colloids and Surfaces A: Physicochemical and Engineering Aspects*. 619, 1–10. https://doi.org/10.1016/j.colsurfa.2021.126544.

Mubarak, N., Faghihzadeh, A., Tan, K., Sahu, J., Abdullah, E., and Jayakumar, N., 2017. Microwave-Assisted Carbon Nanofibers for Removal of Zinc and Copper from Wastewater. *Journal of Nanoscience and Nanotechnology*, 17(3), 1847–1856. http://dx.doi.org/10.1166/jnn.2017.12818.

Nordin, N. A., Abdul Rahman, N., and Abdullah, A. H., 2020. Effective Removal of Pb (II) Ions by Electrospun PAN/Sago Lignin-Based Activated Carbon Nanofibers. *Molecules*, 25(13), 1–21. https://doi.org/10.3390/molecules25133081.

Olufemi, B., and Omolola, E., 2018. Adsorption of Nickel (II) Ions from Aqueous Solution Using Banana Peel and Coconut Shell. *International Journal of Technology*, 9(3), 434–445. https://doi.org/10.14716/ijtech.v9i3.1936.

Ramutshatsha-Makhwedzha, D., Ngila, J. C., Ndungu, P. G., and Nomngongo, P. N., 2019. Ultrasound Assisted Adsorptive Removal of Cr, Cu, Al, Ba, Zn, Ni, Mn, Co and Ti from Seawater Using Fe2O3-SiO2-PAN Nanocomposite: Equilibrium Kinetics. *Journal of Marine Science and Engineering*, 7(5), 1–16. https://doi.org/10.3390/jmse7050133.

Roosta, M., Ghaedi, M., Daneshfar, A., and Sahraei, R., 2014. Experimental Design Based Response Surface Methodology Optimization of Ultrasonic Assisted Adsorption of Safaranin O by Tin Sulfide Nanoparticle Loaded on Activated Carbon. *Spectrochimica Acta Part A: Molecular and Biomolecular Spectroscopy*, 122, 223–231. https://doi.org/10.1016/j.saa.2013.10.116.

Salihi, E. Ç., Wang, J., Coleman, D. J., and Šiller, L., 2016. Enhanced Removal of Nickel (II) Ions from Aqueous Solutions by SDS-Functionalized Graphene Oxide. *Separation science and technology*, 51(8), 1317–1327, http://dx.doi.org/10.1080/01496395.2016.1162172.

Shahriari, T., Mehrdadi, N., and Tahmasebi, M., 2019. Study of Cadmium and Nickel Removal from Battery Industry Wastewater by Fe_2O_3 Nanoparticles. *Pollution*, 5(3), 515–524. https://doi.org/10.22059/poll.2018.268193.530.

Thangaraj, V., Aravamudan, K., Lingam, R., and Subramanian, S., 2019. Individual and Simultaneous Adsorption of Ni (II), Cd (II), And Zn (II) Ions Over Polyamide Resin: Equilibrium, Kinetic and Thermodynamic Studies. *Environmental Progress & Sustainable Energy*, 38(1), S340–S351. http://dx.doi.org/10.1002/ep.13056.

Zafar, S., Khan, M. I., Khraisheh, M., Lashari, M. H., Shahida, S., Azhar, M. F., Prapamonthon, P., Mirza, M. L., and Khalid, N., 2019. Kinetic, Equilibrium and Thermodynamic Studies for Adsorption of Nickel Ions onto Husk of Oryza Sativa. *Desalination and Water Treat*, 167, 277–290. http://dx.doi.org/10.5004/dwt.2019.24646.

Zakaria, A. F., Kamaruzaman, S., and Abdul Rahman, N., 2021. Electrospun Polyacrylonitrile/Lignin/Poly (Ethylene Glycol)–Based Porous Activated Carbon Nanofiber for Removal of Nickel (II) Ion from Aqueous Solution. *Polymers*, 13(20), 3590. https://doi.org/10.3390/polym13203590.

Zhang, X., and Wang, X., 2015. Adsorption and Desorption of Nickel (II) Ions from Aqueous Solution by A Lignocellulose/Montmorillonite Nanocomposite, *PLOS ONE*, 10(2). https://doi.org/10.1371/journal.pone.0117077.